

Finite-element simulation of cavity modes in a micro-fluidic dye ring laser

M. Gersborg-Hansen, S. Balslev, and N. A. Mortensen[§]

NanoDTU, MIC – Department of Micro and Nanotechnology, Technical University of Denmark, DK-2800 Kongens Lyngby, Denmark

Abstract. We consider a recently reported micro-fluidic dye ring laser and study the full wave nature of TE modes in the cavity by means of finite-element simulations. The resonance wave-patterns of the cavity modes support a ray-tracing view and we are also able to explain the spectrum in terms of standing waves with a mode spacing $\delta k = 2\pi/L_{\text{eff}}$ where L_{eff} is the effective optical path length in the cavity.

Submitted to: *J. Opt. A: Pure Appl. Opt.*

[§] Corresponding author: nam@mic.dtu.dk

1. Introduction

Compact, efficient, and on-chip light-sources are of considerable interest for use in lab-on-a-chip applications [1] and recently there has been an increasing effort in realizing micro-fluidic dye lasers based on glass or polymer [2, 3, 4, 5, 6, 7].

Typically, the cavity designs rely on classical ray-tracing arguments rather than full wave simulations. In this paper we consider a geometry resembling that of Refs. [3, 5, 6] and offer a full wave study of the TE modes in the cavity. The resonance wave-patterns of the cavity modes support the ray-tracing view and we are also able to explain the mode-spacing of the spectrum in terms of standing waves.

The paper is organized as follows: In Sec. 2 we present the geometry, in Sec. 3 we address the mode spacing by quasi one-dimensional considerations, in Sec. 4 we numerically solve the wave equation, and in Sec. 5 we discuss aspects of optical gain. Finally, in Sec. 6 conclusions are given.

2. Geometry

We consider the two-dimensional laser resonator illustrated in Fig. 1 which corresponds to the planar cavities studied experimentally in Refs. [3, 5, 6]. The cavity resembles a classical Fabry-Perot resonator and consists of two dielectric isosceles triangles with

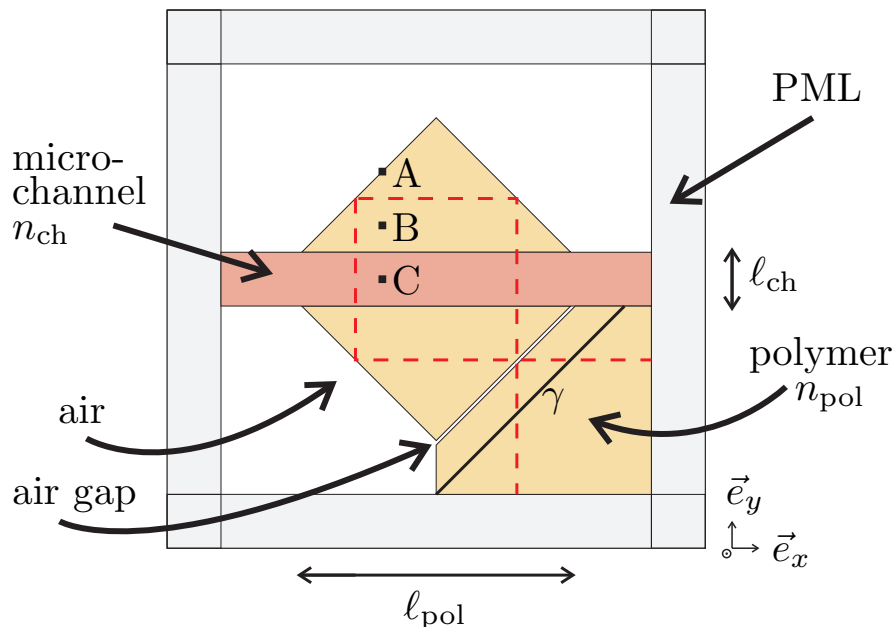


Figure 1. Geometry consisting of a polymer-defined micro-cavity with an embedded micro-fluidic channel containing a dissolved laser dye. Out coupling of power from the cavity occurs through an evanescent-field coupling through an air gap to an adjacent polymer region where the output power is evaluated by an integral along the solid line γ . The dashed line indicates a typical optical path in the cavity. Simulations are carried out for point-source excitations at positions A, B, and C, respectively.

baseline ℓ_{pol} and refractive index n_{pol} separated by a microfluidic channel of width ℓ_{ch} containing a fluid with refractive index n_{ch} . Light is confined to the cavity by total-internal reflections at the polymer-air interfaces at an angle of incidence of $\pi/4$. Out coupling of power occurs through an evanescent-field coupling to an adjacent polymer region. In the experiments in Refs. [5, 6] the microfluidic channel is filled by a dye doped liquid acting as gain medium. In Ref. [5] $\ell_{\text{pol}} \sim 700 \mu\text{m}$, the cavity is pumped at the wavelength $\lambda = 532 \text{ nm}$ by a pulsed frequency doubled Nd:YAG laser, and lasing occurs in the visible around $\lambda \sim 570 \text{ nm}$. For details on the pump power and lasing threshold we refer to Ref. [5].

Throughout the rest of the paper we consider a typical structure with $\ell_{\text{ch}}/\ell_{\text{pol}} = 0.2$ and for the evanescent-field coupling we have $w/\ell_{\text{pol}} \simeq 0.028$ for the width w of the air gap. For the refractive indices we use $n_{\text{pol}} = 1.6$ and $n_{\text{ch}} = 1.43$. These numbers give an index step which is typical for a liquid and a polymer. However, we emphasize that the particular choice of numbers do not affect our overall findings and conclusions.

3. Quasi one-dimensional approach to mode spacing

We first estimate the mode spacing by considering a plane wave travelling around in the cavity, see Fig. 1. In this ray-tracing like approach we neglect reflections at the polymer-fluid interfaces which is justified by the very small Fresnel reflection probability

$$R = \left(\frac{n_{\text{pol}} - n_{\text{ch}}}{n_{\text{pol}} + n_{\text{ch}}} \right)^2 \simeq 0.31 \% \quad (1)$$

We imagine modes somewhat similar to whispering-gallery modes (WGMs) in resonators of circular shape. However, in this case the modes are subject to four total-internal reflections at an incidence angle of $\pi/4$ irrespectively of the mode-index and all modes have the same effective optical path length. Contrary to WGMs these modes have thus no cut-off for decreasing mode index caused by decreasing incidence angle. The accumulated phase during one round-trip of a plane-wave in the ring cavity is

$$\delta\phi = kL_{\text{eff}} + \varphi \quad (2)$$

where $k = 2\pi/\lambda = \omega/c$ is the free-space wave number,

$$L_{\text{eff}} = 2n_{\text{pol}}\ell_{\text{pol}} + 2n_{\text{ch}}\ell_{\text{ch}} \quad (3)$$

is the effective optical path length in the cavity, and

$$\varphi = 4 \times \arg \left(\frac{\cos(\frac{\pi}{4}) - \sqrt{n_{\text{pol}}^{-2} - \sin^2(\frac{\pi}{4})}}{\cos(\frac{\pi}{4}) + \sqrt{n_{\text{pol}}^{-2} - \sin^2(\frac{\pi}{4})}} \right) \quad (4)$$

is the phase picked up during the four total-internal reflections at the polymer-air interfaces at incidence angle of $\pi/4$. The resonance condition is $\delta\phi = 2\pi m$ with the mode-index m being an integer. Obviously, the corresponding modes

$$k_m = \frac{2\pi m - \varphi}{L_{\text{eff}}} \quad (5)$$

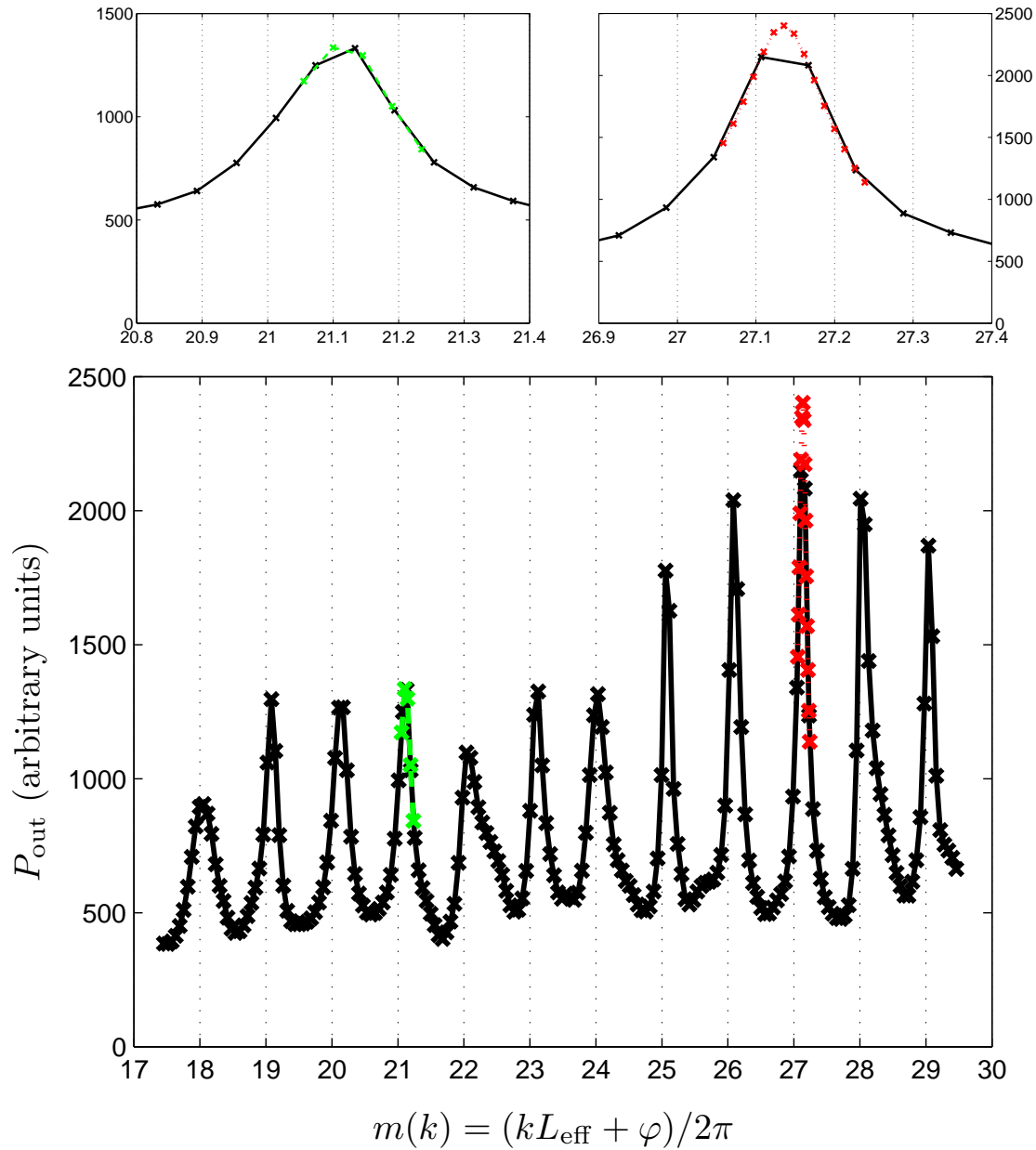


Figure 2. Mode spectrum for a point-source excitation at position A, see Fig. 1. The top panels show close-ups with a higher resolution of the respective peaks at $m \sim 21$ and $m \sim 27$ indicated in the lower panel.

are equally spaced with the mode-spacing

$$\delta k = \frac{2\pi}{L_{\text{eff}}}. \quad (6)$$

4. Two-dimensional wave equation approach

The full wave nature is governed by the wave equation [8]

$$\nabla \times \nabla \times \vec{E}(\vec{r}) = \epsilon(\vec{r})k^2\vec{E}(\vec{r}) \quad (7)$$

where \vec{E} is the electrical field and $\epsilon(\vec{r}) = n^2(\vec{r})$ is the dielectric function. We solve the wave equation in a planar geometry for TE modes, i.e. $\vec{E}(\vec{r}) = E_z(\vec{r})\vec{e}_z$ and $\vec{r} = x\vec{e}_x + y\vec{e}_y$. For the simulations we employ a finite-element method [9] with "open" boundary conditions taken into account by perfectly matching layers (PMLs) at the edges of the simulation domain [10], see Fig. 1. This allows outgoing waves with negligible back reflection.

We solve Eq. (7) subject to a point-source excitation and modes are monitored by calculating the output power $P_{\text{out}}(k)$ by integration along γ in the polymer region adjacent to the cavity, see Fig. 1, for different values of k . The point-source has the appealing feature that it radiates isotropically in a homogeneous space and thus it will in general excite the full spectrum of cavity eigenmodes (except of course from the statistically few having a true node at the exact position of the point-source).

In order to compare to the predicted mode spectrum, we have transformed the k values into a mode index

$$m(k) = (kL_{\text{eff}} + \varphi)/2\pi \quad (8)$$

and according to Eq. (5) we expect $P_{\text{out}}(m)$ to have resonances centred at integer values of m . Fig. 2 illustrates this in the case of a point-source excitation at point A, see Fig. 1.

The over-all agreement between the full wave simulation and the quasi one-dimensional model is excellent, but from Fig. 2 it is also clear that the different peaks are slightly blue-shifted from integer values. The top panels illustrate this for two of the peaks indicated by green and red in the lower panel. This small shift may originate in a slightly modified phase shift at the edge with evanescent field coupling compared to the three other edges of the cavity. The small Fresnel reflection may also slightly modify the spectrum compared to the results derived from the quasi one-dimensional model.

Figure 2 shows results in the range from $m \sim 18$ up to $m \sim 29$. When further increasing m the pattern of peaks persist with a small tendency that the peaks sharpen. This trend has been investigated up $m \sim 100$ where simulations turn highly computationally demanding (results not shown). However, since the quasi one-dimensional interpretation does not support a cut-off for increasing m we believe that a spectrum of equally spaced modes persist for increasing m .

For decreasing m WGMs will typically experience a cut-off because the angles of incidence at some point do not support total-internal reflection. However, as discussed for the quasi one-dimensional model the particular class of modes in the present cavity do not share this property. In fact, in the simulations we have observed the modes down to $m \sim 10$ below which pronounced deviations from the quasi one-dimensional predictions start to emerge. Deviations most likely appear because the polymer-air interface has spatial variations on a length scale comparable to the wavelength of the light. In other

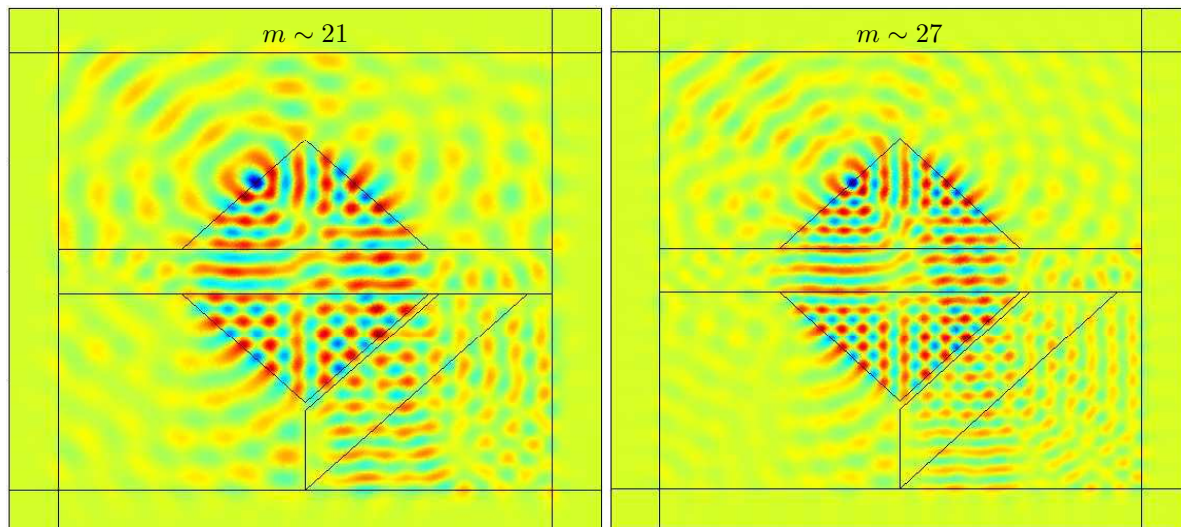


Figure 3. Electrical fields at $m(k) = 21.1000$ and $m(k) = 27.1355$ for a point-source excitation at position A, see Fig. 1.

words, the ray-tracing picture fails and concepts like total-internal reflection derived from Snell's law do not accurately capture the true wave physics.

In order to verify that the peaks in Fig. 2 really do correspond to cavity modes we have studied the corresponding electrical fields at resonance, see Fig. 3. These fields resemble pure eigenfunctions of the resonator while off-resonance fields correspond to linear combinations of a larger number of eigenfunctions. Starting from e.g. the source point, the number of oscillations along one round trip equals m in full agreement with the quasi one-dimensional arguments.

When the cavity is excited at different positions the overall output spectrum is the same such that peaks remain unshifted while changes are observed in the intensity distribution only. The reason is that different positions of the source will excite different linear combinations of eigenmodes (being correlated with the intensity level) while the eigenspectrum itself (being correlated with the resonance positions) remains unchanged. In Fig. 4 we illustrate this for different positions of the point source. The spectrum also reveals structure, though very broad with low intensity, in between integer values of $m(k)$. This structure also corresponds to quasi eigenmodes which however are much more poorly confined to the cavity compared to the well-confined modes with integer values of $m(k)$.

5. Optical gain medium

Lasing of course relies on the presence of an optical gain medium. In Refs. [3, 5] dissolved laser dye in the microfluidic channel provides the gain. While the dynamics of lasing is difficult to address we may with little effort investigate the influence of gain on the mode spectrum. The present numerical model allows for such investigations, but for low

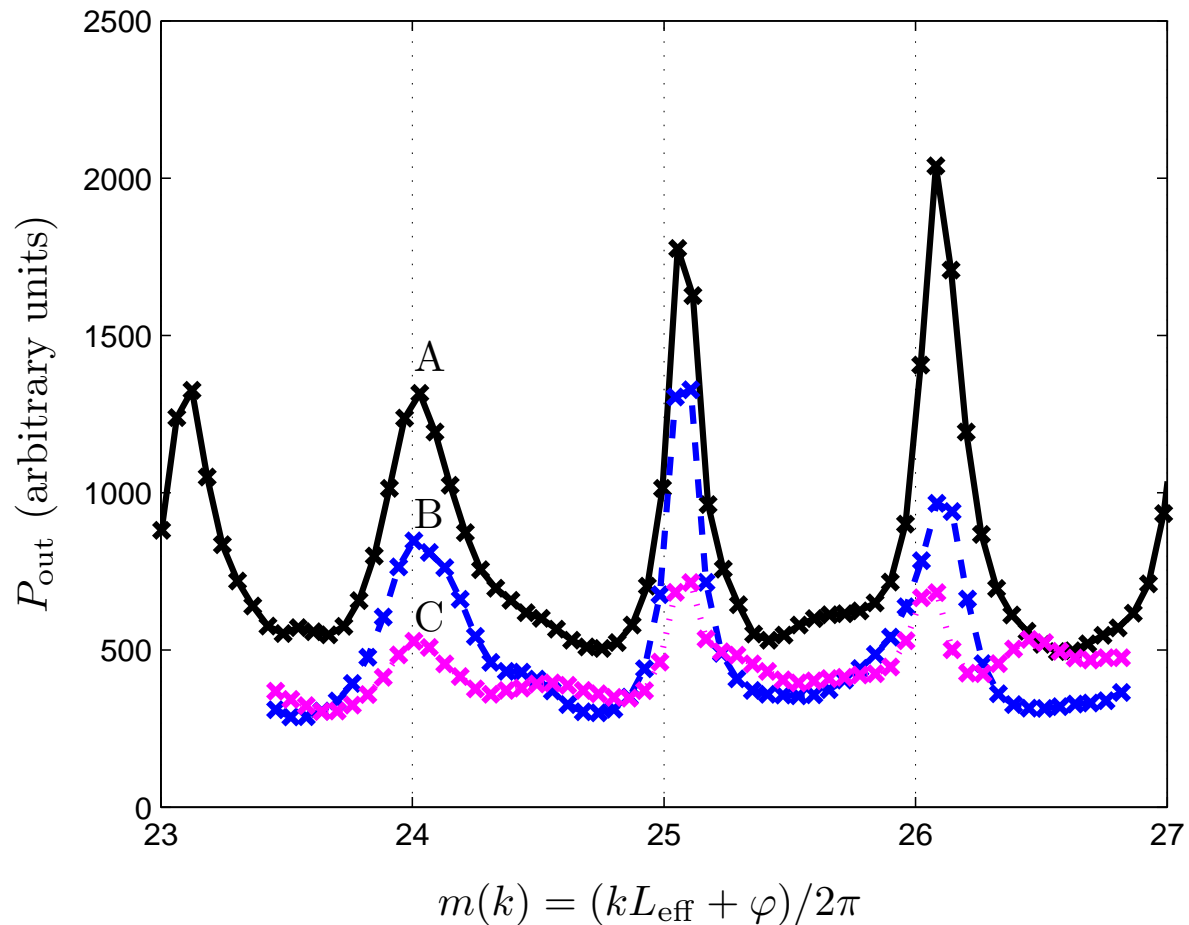


Figure 4. Mode spectra for point-source excitation at positions A, B, and C, see Fig. 1.

concentrations general trends may be more easily analyzed with the aid of perturbation theory [11]. Doping by e.g. Rhodamine 6G (Rh6G), as in the experiment [5], will change the refractive index in the channel accordingly, i.e. $n_{\text{ch}} \rightarrow n_{\text{ch}} + n_{\text{Rh6G}}$ where for the latter $n_{\text{Rh6G}} = n'_{\text{Rh6G}} + in''_{\text{Rh6G}}$. In the case of $n''_{\text{Rh6G}} \ll n'_{\text{Rh6G}} \ll n_{\text{ch}}$ we get

$$\Delta k = -\frac{k}{2} \frac{\langle \vec{E} | \Delta \epsilon | \vec{E} \rangle}{\langle \vec{E} | \epsilon | \vec{E} \rangle}, \quad \Delta \epsilon = (n_{\text{ch}} + n_{\text{Rh6G}})^2 - n_{\text{ch}}^2 \simeq (n'_{\text{Rh6G}})^2 \quad (9)$$

from which we expect a red-shift of the modes of the order $\Delta k \propto (n'_{\text{Rh6G}})^2 k$ along with a narrowing of the modes. A blue-shift may be observed in the case where $n''_{\text{Rh6G}} > \sqrt{n'_{\text{Rh6G}}(n'_{\text{Rh6G}} + n_{\text{ch}})}$.

6. Discussion and conclusion

In this work we have used finite-element simulations to study the cavity mode spectrum of a micro-fluidic dye ring laser with a planar geometry resembling the one studied experimentally in Refs. [3, 5]. We have performed a full wave study of the TE modes

in the cavity and found very good agreement with a quasi one-dimensional plane wave description with resonances corresponding to standing waves.

In principle our simulations allow for an estimate of the quality factor of the modes, but realistic simulations for the experimental device require more details to be taken into account. For instance one would need to include the three-dimensional nature of the device to describe the radiation field accurately and the details of the evanescent field coupling would also influence the quality factor. Such issues add to the difficulty in addressing the dynamics of lasing so in this work we have only addressed the passive device. However, we have estimated a doping-induced shift of the spectrum by perturbative means.

In the simulations we have considered mode-indices $m(k)$ up to around 100 while in the experiments the corresponding typical mode index is estimated to be around two orders of magnitude larger. Nevertheless, we are confident that the standing-wave interpretation may be safely extrapolated to the experimental regime [3, 5, 6] due to the scale invariance of the wave equation [8] and the fact that this class of modes has no cut-off with respect to increasing mode index.

Acknowledgment

We thank A. Kristensen for stimulating discussions. The work was supported by the Danish Technical Research Council (STVF, grant no. 26-02-0064).

- [1] Verpoorte E 2003 *Lab Chip* **3** 42N – 52N
- [2] Helbo B, Kristensen A and Menon A 2003 *J. Micromech. Microeng.* **13** 307 – 311
- [3] Cheng Y, Sugioka K and Midorikawa K 2004 *Opt. Lett.* **29** 2007 – 2009
- [4] Balslev S and Kristensen A 2005 *Opt. Express* **13** 344 – 351
- [5] Gersborg-Hansen M, Balslev S, Mortensen N A and Kristensen A 2005 *Microelectron. Eng.* **78-79** 185 – 189
- [6] Galas J C, Torres J, Belotti M, Kou Q and Chen Y 2005 *Appl. Phys. Lett.* **86**
- [7] Vezenov D V, Mayers B T, Conroy R S, Whitesides G M, Snee P T, Chan Y, Nocera D G and Bawendi M G 2005 *J. Am. Chem. Soc.* **127** 8952 – 8953
- [8] Joannopoulos J D, Meade R D and Winn J N 1995 *Photonic Crystals: Molding the Flow of Light* (Princeton: Princeton University Press)
- [9] Comsol support and Femlab documentation, www.comsol.com
- [10] Jin J 2002 *The Finite Element Method in Electromagnetics* (New York: Wiley-IEEE press) 2 ed.
- [11] Johnson S G, Ibanescu M, Skorobogatiy M A, Weisberg O, Joannopoulos J D and Fink Y 2002 *Phys. Rev. E* **65** 066611